
SUNY Institute of Technology at Utica/Rome
Conference on Theoretical High Energy Physics

June 6th, 2002

Gaussian Sum-Rules, Scalar Gluonium, and Instantons

T.G. STEELE ^{a, 1}, D. HARNETT ^a,
G. ORLANDINI ^b,

^a *Department of Physics & Engineering Physics, University of Saskatchewan, Saskatoon,
Saskatchewan, S7N 5E2, Canada*

^b *Dipartimento di Fisica and INFN Gruppo Collegato di Trento, Università di Trento,
I-38050 Povo, Italy*

Abstract

Gaussian sum-rules relate a QCD prediction to a two-parameter Gaussian-weighted integral of a hadronic spectral function, providing a clear conceptual connection to quark-hadron duality. In contrast to Laplace sum-rules, the Gaussian sum-rules exhibit enhanced sensitivity to excited states of the hadronic spectral function. The formulation of Gaussian sum-rules and associated analysis techniques for extracting hadronic properties from the sum-rules are reviewed and applied to scalar gluonium. With the inclusion of instanton effects, the Gaussian sum-rule analysis results in a consistent scenario where the gluonic resonance strength is spread over a broad energy range below 1.6 GeV, and indicates the presence of gluonium content in more than one hadronic state.

¹Electronic address: Tom.Steele@usask.ca

1 Introduction

The hadronic spectrum has too many scalar states above 1 GeV for a $q\bar{q}$ nonet, as would be anticipated if gluonium states exist in the 1–2 GeV region [1]. Determining how this gluonium content is distributed among these scalar-isoscalar resonances is thus an important issue. In particular, the possibility that the observed hadronic states are mixtures of gluonium and quark mesons must be explored.

Gaussian sum-rules are sensitive to the hadronic spectral function over a wide energy range, and are thus well-suited to studying the distribution of gluonium states. The simplest Gaussian sum-rule (GSR) [2]

$$G(\hat{s}, \tau) = \frac{1}{\pi} \int_{t_0}^{\infty} \frac{1}{\sqrt{4\pi\tau}} \exp\left(-\frac{(t - \hat{s})^2}{4\tau}\right) \rho(t) dt \quad , \quad \tau > 0 \quad (1)$$

relates a QCD prediction on the left-hand side of (1) to the hadronic spectral function $\rho(t)$ (with physical threshold t_0) smeared over the energy range $\hat{s} - 2\sqrt{\tau} \lesssim t \lesssim \hat{s} + 2\sqrt{\tau}$, representing an energy interval for quark-hadron duality. An interesting aspect of the GSR is that the duality interval is constrained by QCD. A lower bound on this duality scale τ necessarily exists because the QCD prediction has renormalization-group properties that reference running quantities to the energy scale $\nu^2 = \sqrt{\tau}$ [2, 3]. Thus it is not possible to achieve the formal $\tau \rightarrow 0$ limit where complete knowledge of the spectral function could be obtained via

$$\lim_{\tau \rightarrow 0} G(\hat{s}, \tau) = \frac{1}{\pi} \rho(\hat{s}) \quad , \quad \hat{s} > t_0 \quad . \quad (2)$$

However, there is no theoretical constraint on the quantity \hat{s} representing the peak of the Gaussian kernel appearing in (1). Thus the \hat{s} dependence of the QCD prediction $G(\hat{s}, \tau)$ probes the behaviour of the smeared spectral function, reproducing the essential features of the spectral function. In particular, as \hat{s} passes through t values corresponding to resonance peaks, the Gaussian kernel in (1) reaches its maximum value, implying that Gaussian sum-rules weight excited and ground states equally. This behaviour should be contrasted with Laplace sum-rules

$$R(\Delta^2) = \frac{1}{\pi} \int_{t_0}^{\infty} \exp\left(-\frac{t}{\Delta^2}\right) \rho(t) dt \quad , \quad (3)$$

where excited states are damped by the exponential decay of the Laplace kernel. Thus, in comparison with Laplace sum-rules the Gaussian sum-rule (GSR) has an enhanced sensitivity to excited states of the spectral function.

In this paper, the original formulation of Gaussian sum-rules [2] and analysis techniques for extracting spectral function hadronic features [3, 4] will be reviewed. These techniques will then be applied to scalar gluonium, where instanton contributions are known to be crucial for a consistent Laplace sum-rule analysis [5, 6]. Results of the GSR analysis indicate that the gluonium spectral strength is distributed across a broad energy range below 1.6 GeV [4].

2 Foundations of Gaussian Sum-Rules

The general formulation of GSRs will be reviewed in the context of scalar gluonium probed by the following correlation function.

$$\Pi(Q^2) = i \int d^4x e^{iq \cdot x} \langle O | T \{ J(x), J(0) \} | O \rangle \quad , \quad Q^2 = -q^2 \quad (4)$$

$$J(x) = -\frac{\pi^2}{\alpha\beta_0} \beta(\alpha) G_{\mu\nu}^a(x) G^{a\mu\nu}(x) \quad , \quad G_{\mu\nu}^a = \partial_\mu A_\nu^a - \partial_\nu A_\mu^a + gf^{abc} A_\mu^b A_\nu^c \quad (5)$$

$$\beta(\alpha) = \nu^2 \frac{d}{d\nu^2} \left(\frac{\alpha(\nu)}{\pi} \right) = -\beta_0 \left(\frac{\alpha}{\pi} \right)^2 - \beta_1 \left(\frac{\alpha}{\pi} \right)^3 + \dots \quad (6)$$

$$\beta_0 = \frac{11}{4} - \frac{1}{6}n_f \quad , \quad \beta_1 = \frac{51}{8} - \frac{19}{24}n_f \quad , \quad \dots \quad (7)$$

The current $J(x)$ is renormalization-group invariant in the chiral limit of n_f massless quarks as needed to probe physical (renormalization-group invariant) hadronic states.

From the asymptotic form and assumed analytic properties of (4) follows a dispersion relation with three subtraction constants

$$\Pi(Q^2) - \Pi(0) = Q^2 \Pi'(0) + \frac{1}{2} Q^4 \Pi''(0) - \frac{Q^6}{\pi} \int_{t_0}^{\infty} \frac{\rho(t)}{t^3(t+Q^2)} dt \quad , \quad Q^2 > 0 \quad (8)$$

where $\rho(t)$ is the hadronic spectral function with physical threshold t_0 , and the subtraction constant $\Pi(0)$ has been included on the side of the equation containing the QCD prediction because it is determined by the low-energy theorem [7]

$$\Pi(0) \equiv \lim_{Q^2 \rightarrow 0} \Pi(Q^2) = \frac{8\pi}{\beta_0} \langle J \rangle \quad . \quad (9)$$

The undetermined subtraction constants $\Pi'(0)$ and $\Pi''(0)$ and field-theoretical divergences in $\Pi(Q^2)$ proportional to Q^4 are eliminated in an integer-weighted family of Gaussian sum-rules¹

$$G_k(\hat{s}, \tau) \equiv \sqrt{\frac{\tau}{\pi}} \mathcal{B} \left\{ \frac{(\hat{s} + i\Delta)^k \Pi(-\hat{s} - i\Delta) - (\hat{s} - i\Delta)^k \Pi(-\hat{s} + i\Delta)}{i\Delta} \right\} \quad (10)$$

where $k = -1, 0, 1, \dots$ and with the Borel transform \mathcal{B} defined by

$$\mathcal{B} \equiv \lim_{\substack{N, \Delta^2 \rightarrow \infty \\ \Delta^2/N \equiv 4\tau}} \frac{(-\Delta^2)^N}{\Gamma(N)} \left(\frac{d}{d\Delta^2} \right)^N \quad . \quad (11)$$

Applying definition (10) to both sides of (8) annihilates the undetermined low-energy constants and the field theoretical divergence contained in $\Pi(Q^2)$. Using the identity

$$\mathcal{B} \left[\frac{(\Delta^2)^n}{\Delta^2 + a} \right] = \frac{1}{4\tau} (-a)^n \exp \left(\frac{-a}{4\tau} \right) \quad \text{for } n \geq 0 \quad , \quad (12)$$

¹This definition is a natural generalization of that given in [2]. To recover the original Gaussian sum-rule, we simply let $k = 0$ in (10).

then leads to the following GSR family:

$$G_k(\hat{s}, \tau) + \delta_{k-1} \frac{1}{\sqrt{4\pi\tau}} \exp\left(\frac{-\hat{s}^2}{4\tau}\right) \Pi(0) = \int_{t_0}^{\infty} t^k \exp\left[\frac{-(\hat{s}-t)^2}{4\tau}\right] \frac{1}{\pi} \rho(t) dt \quad (13)$$

Calculation of the Borel transform is achieved through an identity relating (11) to the inverse Laplace transform [2]

$$\mathcal{B}[f(\Delta^2)] = \frac{1}{4\tau} \mathcal{L}^{-1}[f(\Delta^2)] \quad (14)$$

where, in our notation,

$$\mathcal{L}^{-1}[f(\Delta^2)] = \frac{1}{2\pi i} \int_{a-i\infty}^{a+i\infty} f(\Delta^2) \exp\left(\frac{\Delta^2}{4\tau}\right) d\Delta^2 \quad (15)$$

with a chosen such that all singularities of f lie to the left of a in the complex Δ^2 -plane. With a change of variables, the calculation of the GSR reduces to [4]

$$G_k(\hat{s}, \tau) = \frac{1}{\sqrt{4\pi\tau}} \frac{1}{2\pi i} \int_{\Gamma_1 + \Gamma_2} (-w)^k \exp\left[\frac{-(\hat{s}+w)^2}{4\tau}\right] \Pi(w) dw \quad (16)$$

where Γ_1 and Γ_2 are the parabolae depicted in Figure 1.

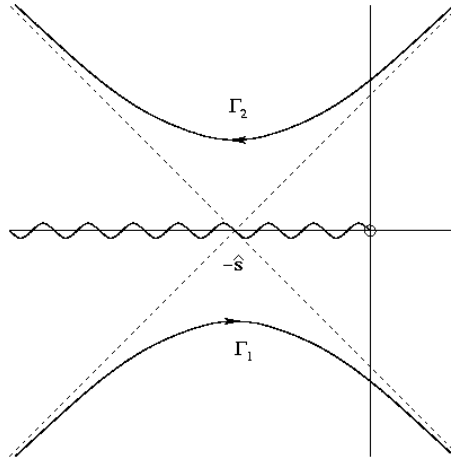


Figure 1: Contour of integration $\Gamma_1 + \Gamma_2$ defining the Gaussian sum-rule. The wavy line on the negative real axis denotes the branch cut of $\Pi(z)$.

3 Normalized Gaussian Sum-Rules

Studies of Gaussian sum-rules have traditionally focussed on their connection with finite-energy sum-rules as established through the diffusion equation

$$\frac{\partial^2 G_k(\hat{s}, \tau)}{\partial \hat{s}^2} = \frac{\partial G_k(\hat{s}, \tau)}{\partial \tau} \quad (17)$$

In particular, the resonance(s) plus continuum model

$$\rho(t) = \rho^{\text{had}}(t) + \theta(t - s_0) \text{Im}\Pi^{\text{QCD}}(t) \quad , \quad (18)$$

when $\rho^{\text{had}}(t)$ is evolved through the diffusion equation (17), only reproduces the QCD prediction at large energies (τ large) if the resonance and continuum contributions are balanced through the finite-energy sum-rules [2]

$$F_n(s_0) = \frac{1}{\pi} \int_{t_0}^{s_0} t^n \rho^{\text{had}}(t) dt \quad , \quad n = \text{integer} \quad . \quad (19)$$

Within the resonance(s) plus continuum model (18), the continuum contribution to the GSRs is determined by QCD

$$G_k^{\text{cont}}(\hat{s}, \tau, s_0) = \frac{1}{\sqrt{4\pi\tau}} \int_{s_0}^{\infty} t^k \exp\left[\frac{-(\hat{s} - t)^2}{4\tau}\right] \frac{1}{\pi} \text{Im}\Pi^{\text{QCD}}(t) dt \quad , \quad (20)$$

and is thus combined with $G_k(\hat{s}, \tau)$ to give the total QCD contribution

$$G_k^{\text{QCD}}(\hat{s}, \tau, s_0) \equiv G_k(\hat{s}, \tau) - G_k^{\text{cont}}(\hat{s}, \tau, s_0) \quad , \quad (21)$$

resulting in the final relation between the QCD and hadronic sides of the GSRs.

$$G_k^{\text{QCD}}(\hat{s}, \tau, s_0) + \delta_{k-1} \frac{1}{\sqrt{4\pi\tau}} \exp\left(\frac{-\hat{s}^2}{4\tau}\right) \Pi(0) = \int_{t_0}^{\infty} t^k \exp\left[\frac{-(\hat{s} - t)^2}{4\tau}\right] \frac{1}{\pi} \rho^{\text{had}}(t) dt \quad (22)$$

Integrating both sides of (22) reveals that the normalization of the GSRs is related to the finite-energy sum-rules

$$\int_{-\infty}^{\infty} G_k^{\text{QCD}}(\hat{s}, \tau, s_0) d\hat{s} + \delta_{k-1} \Pi(0) = \frac{1}{\pi} \int_{t_0}^{\infty} t^k \rho^{\text{had}}(t) dt \quad . \quad (23)$$

Thus the diffusion equation analysis [2] relates the normalization of the GSR to the finite-energy sum-rules. Information independent of this relation is extracted from the normalized GSRs

$$N_k^{\text{QCD}}(\hat{s}, \tau, s_0) \equiv \frac{G_k^{\text{QCD}}(\hat{s}, \tau, s_0) + \delta_{k-1} \frac{1}{\sqrt{4\pi\tau}} \exp\left(\frac{-\hat{s}^2}{4\tau}\right) \Pi(0)}{M_{k,0}^{\text{QCD}}(\tau, s_0) + \delta_{k-1} \Pi(0)} \quad (24)$$

$$M_{k,n}(\tau, s_0) = \int_{-\infty}^{\infty} \hat{s}^n G_k(\hat{s}, \tau, s_0) d\hat{s} \quad , \quad n = 0, 1, 2, \dots \quad , \quad (25)$$

which are related to the hadronic spectral function via

$$N_k^{\text{QCD}}(\hat{s}, \tau, s_0) = \frac{\frac{1}{\sqrt{4\pi\tau}} \int_{t_0}^{\infty} t^k \exp\left[\frac{-(\hat{s} - t)^2}{4\tau}\right] \frac{1}{\pi} \rho^{\text{had}}(t) dt}{\int_{t_0}^{\infty} t^k \frac{1}{\pi} \rho^{\text{had}}(t) dt} \quad . \quad (26)$$

4 Gaussian Sum-Rule Analysis Techniques

In the single narrow resonance model, $\rho^{\text{had}}(t)$ takes the form

$$\rho^{\text{had}}(t) = \pi f^2 \delta(t - m^2) \quad (27)$$

where m and f are respectively the resonance mass and coupling. With such an ansatz, the normalized Gaussian sum-rule (26) becomes

$$N_k^{\text{QCD}}(\hat{s}, \tau, s_0) = \frac{1}{\sqrt{4\pi\tau}} \exp \left[-\frac{(\hat{s} - m^2)^2}{4\tau} \right] . \quad (28)$$

Deviations from the narrow-width limit are proportional to $m^2\Gamma^2/\tau$, so this narrow-width model may actually be a good numerical approximation. Phenomenological analysis of the single narrow resonance model proceeds from the observation that (28) has a maximum value (peak) at $\hat{s} = m^2$ independent of the value of τ . The value of s_0 is then optimized by minimizing the τ dependence of the \hat{s} peak position of the QCD prediction, and the resulting τ -averaged \hat{s} peak position leads to a prediction of the resonance mass [3].

The ρ meson illustrates this single-resonance analysis technique and demonstrates that GSRs can be used to predict resonance properties. The correlation function of the vector-isovector correlation function results in the following ($k = 0$) GSR

$$\begin{aligned} G_0^{\text{QCD}}(\hat{s}, \tau, s_0) = & \frac{1}{16\pi^2} \left(1 + \frac{\alpha(\sqrt{\tau})}{\pi} \right) \left[\text{erf} \left(\frac{\hat{s}}{2\sqrt{\tau}} \right) + \text{erf} \left(\frac{s_0 - \hat{s}}{2\sqrt{\tau}} \right) \right] \\ & - \frac{\hat{s}}{32\pi^2\tau\sqrt{\pi\tau}} \exp \left(-\frac{\hat{s}^2}{4\tau} \right) \langle C_4^v \mathcal{O}_4^v \rangle \\ & + \frac{1}{64\pi^2\tau\sqrt{\pi\tau}} \left(-1 + \frac{\hat{s}^2}{2\tau} \right) \exp \left(-\frac{\hat{s}^2}{4\tau} \right) \langle C_6^v \mathcal{O}_6^v \rangle \\ & - \frac{\hat{s}}{128\pi^2\tau^2\sqrt{\pi\tau}} \left(-1 + \frac{\hat{s}^2}{6\tau} \right) \exp \left(-\frac{\hat{s}^2}{4\tau} \right) \langle C_8^v \mathcal{O}_8^v \rangle , \end{aligned}$$

where

$$\langle C_4^v \mathcal{O}_4^v \rangle = \frac{\pi}{3} \langle \alpha G^2 \rangle - 8\pi^2 m \langle \bar{q}q \rangle \quad (29)$$

$$\langle C_6^v \mathcal{O}_6^v \rangle = -\frac{896}{81} \pi^3 \alpha (\langle \bar{q}q \rangle)^2 \quad (30)$$

and $SU(2)$ symmetry along with the vacuum saturation hypothesis have been employed. For brevity, we refer to the literature [8] for the expressions for the dimension eight condensates, and simply use (29) to establish a convention consistent with [9]. Note that the running coupling is referenced to the energy scale $\sqrt{\tau}$, a point which will be discussed in the next Section.

The non-perturbative QCD condensate contributions in (29) are exponentially suppressed for large \hat{s} . Since \hat{s} represents the location of the Gaussian peak on the phenomenological side of the sum-rule, the non-perturbative corrections are most important

in the low-energy region, as anticipated by the role of QCD condensates in relation to the vacuum properties of QCD. This explicit low-energy role of the QCD condensates clearly exhibited for the Gaussian sum-rules is obscured in the Laplace sum-rules.

The QCD inputs used for the ρ meson analysis analysis are

$$\Lambda^{(3)} = 300 \text{ MeV} \quad (31)$$

$$\langle \alpha G^2 \rangle = (0.045 \pm 0.014) \text{ GeV}^4, \quad 2m \langle \bar{q}q \rangle = -f_\pi^2 m_\pi^2 \quad (32)$$

$$\langle C_6^v \mathcal{O}_6^v \rangle = -f_{vs} \frac{896}{81} \pi^3 (1.8 \times 10^{-4} \text{ GeV}^6), \quad f_{vs} = 1.5 \pm 0.5 \quad (33)$$

$$\langle C_8^v \mathcal{O}_8^v \rangle = (0.40 \pm 0.16) \text{ GeV}^8, \quad (34)$$

consistent with the condensate parameters in [9]. The criteria of τ stability of \hat{s} peak predicts the following values for m_ρ and s_0 [3]

$$m_\rho = (0.75 \pm 0.07) \text{ GeV}, \quad s_0 = (1.2 \pm 0.2) \text{ GeV}^2 \quad (35)$$

in excellent agreement with the known value of the ρ mass. Furthermore, the phenomenological and QCD sides of the (normalized) Gaussian sum-rules shown in Figure 2 are in superb agreement even for very small values of τ [3]. This agreement is particularly impressive since there are no free parameters corresponding to the normalization of the curves in this analysis.

In more complicated resonance models, the \hat{s} peak position of the phenomenological model begins to develop τ dependence which is well-described by [3, 4]

$$\hat{s}_{peak}(\tau, s_0) = A + \frac{B}{\tau} + \frac{C}{\tau^2}. \quad (36)$$

Analysis of how the \hat{s} peak “drifts” with τ in comparison with the behaviour (36) then allows optimization of s_0 . After optimization of s_0 , the resonance model parameters are extracted from various moments of the GSRs. For example, a square pulse² centred at $t = m^2$ with total width $2m\Gamma$ leads to the following ($k = 0$) normalized GSR [4]

$$N_0^{\text{QCD}}(\hat{s}, \tau, s_0) = \frac{1}{4m\Gamma} \left[\text{erf} \left(\frac{\hat{s} - m^2 + m\Gamma}{2\sqrt{\tau}} \right) - \text{erf} \left(\frac{\hat{s} - m^2 - m\Gamma}{2\sqrt{\tau}} \right) \right]. \quad (37)$$

Expansion of (37) for small Γ demonstrates that deviations from the narrow width limit (28) scale as $m^2\Gamma^2/\tau$. The resonance parameters can then be determined by the following moment combinations [see (25)] of the right-hand side of (37) [4]

$$\frac{M_{0,1}}{M_{0,0}} = m^2 \quad (38)$$

$$\sigma_0^2 - 2\tau \equiv \frac{M_{0,2}}{M_{0,0}} - \left(\frac{M_{0,1}}{M_{0,0}} \right)^2 = \frac{1}{3} m^2 \Gamma^2, \quad (39)$$

²This model would describe a broad, structureless feature in the hadronic spectral function.

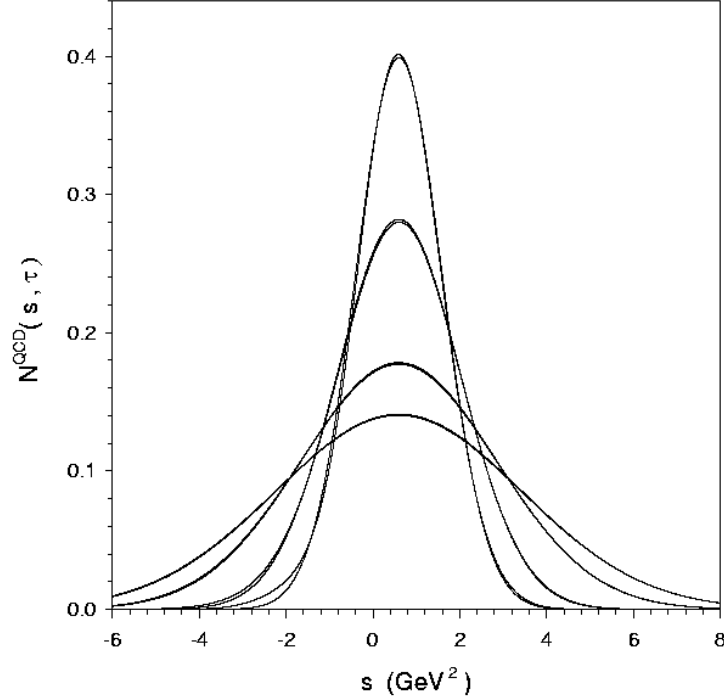


Figure 2: Comparison of the vector-current theoretical prediction for $N_0^{\text{QCD}}(\hat{s}, \tau, s_0)$ with the single resonance phenomenological model. The τ values used for the four pairs of curves, from top to bottom in the figure, are respectively $\tau = 0.5 \text{ GeV}^4$, $\tau = 1.0 \text{ GeV}^4$, $\tau = 2.5 \text{ GeV}^4$, and $\tau = 4.0 \text{ GeV}^4$. Note the almost complete overlap between the QCD prediction and phenomenological model.

where it is understood that the QCD expressions at the optimized value of s_0 are used on the left-hand side.³

Moments also provide a method for testing the accuracy of agreement between the QCD and phenomenological sides of the normalized GSR beyond a simple χ^2 measure which could be extracted from plots such as Figure 2. For example, a combination of third-order moments representing the asymmetry of the \hat{s} dependence about its average value results in [4]

$$A_0^{(3)} = \frac{M_{0,3}}{M_{0,0}} - 3 \left(\frac{M_{0,2}}{M_{0,0}} \right) \left(\frac{M_{0,1}}{M_{0,0}} \right) + 2 \left(\frac{M_{0,1}}{M_{0,0}} \right)^3 = 0 \quad , \quad (40)$$

and hence a deviation of the QCD value of this moment from its value of $A_0^{(3)} = 0$ in the square pulse model indicates a shortcoming of the model spectral function in comparison with QCD.

³The residual moment combinations leading to the resonance parameters must be τ independent, providing a consistency check on the analysis. Weak residual τ dependence is averaged over the τ range used to extract the optimized s_0 from the peak-drift analysis.

The procedure for studying an N -parameter resonance model is easily generalized. The peak-drift analysis is used to optimize s_0 , the lowest N moments are used to determine the resonance model parameters, and the next-highest moment combination is employed as a test of the accuracy of the model's agreement with the QCD prediction.

5 Scalar Gluonium Gaussian Sum-Rules

The lowest two Gaussian sum-rules for scalar gluonium contain perturbative, condensate and instanton corrections, and are given by [4]

$$\begin{aligned}
G_{-1}^{\text{QCD}}(\hat{s}, \tau, s_0) = & -\frac{1}{\sqrt{4\pi\tau}} \int_0^{s_0} t \, dt \exp \left[\frac{-(\hat{s} - t)^2}{4\tau} \right] \left[(a_0 - \pi^2 a_2) + 2a_1 \log \left(\frac{t}{\nu^2} \right) \right. \\
& \left. + 3a_2 \log^2 \left(\frac{t}{\nu^2} \right) \right] \\
& + \frac{1}{\sqrt{4\pi\tau}} \exp \left(\frac{-\hat{s}^2}{4\tau} \right) \left[-b_0 \langle J \rangle + \frac{c_0 \hat{s}}{2\tau} \langle \mathcal{O}_6 \rangle - \frac{d_0}{4\tau} \left(\frac{\hat{s}^2}{2\tau} - 1 \right) \langle \mathcal{O}_8 \rangle \right] \\
& - \frac{16\pi^3}{\sqrt{4\pi\tau}} \int \text{dn}(\rho) \rho^4 \int_0^{s_0} t \exp \left[\frac{-(\hat{s} - t)^2}{4\tau} \right] J_2(\rho\sqrt{t}) Y_2(\rho\sqrt{t}) \, dt \\
& - \frac{128\pi^2}{\sqrt{4\pi\tau}} \exp \left(\frac{-\hat{s}^2}{4\tau} \right) \int \text{dn}(\rho)
\end{aligned} \tag{41}$$

$$\begin{aligned}
G_0^{\text{QCD}}(\hat{s}, \tau, s_0) = & -\frac{1}{\sqrt{4\pi\tau}} \int_0^{s_0} t^2 \, dt \exp \left[\frac{-(\hat{s} - t)^2}{4\tau} \right] \left[(a_0 - \pi^2 a_2) + 2a_1 \log \left(\frac{t}{\nu^2} \right) \right. \\
& \left. + 3a_2 \log^2 \left(\frac{t}{\nu^2} \right) \right] \\
& - \frac{1}{\sqrt{4\pi\tau}} b_1 \langle J \rangle \int_0^{s_0} \exp \left[\frac{-(\hat{s} - t)^2}{4\tau} \right] \, dt \\
& + \frac{1}{\sqrt{4\pi\tau}} \exp \left(\frac{-\hat{s}^2}{4\tau} \right) \left[c_0 \langle \mathcal{O}_6 \rangle - \frac{d_0 \hat{s}}{2\tau} \langle \mathcal{O}_8 \rangle \right] \\
& - \frac{16\pi^3}{\sqrt{4\pi\tau}} \int \text{dn}(\rho) \rho^4 \int_0^{s_0} t^2 \exp \left[\frac{-(\hat{s} - t)^2}{4\tau} \right] J_2(\rho\sqrt{t}) Y_2(\rho\sqrt{t}) \, dt \quad .
\end{aligned} \tag{42}$$

The perturbative coefficients in these expressions are

$$a_0 = -2 \left(\frac{\alpha}{\pi} \right)^2 \left[1 + \frac{659}{36} \frac{\alpha}{\pi} + 247.480 \left(\frac{\alpha}{\pi} \right)^2 \right] \tag{43}$$

$$a_1 = 2 \left(\frac{\alpha}{\pi} \right)^3 \left[\frac{9}{4} + 65.781 \frac{\alpha}{\pi} \right] \quad , \quad a_2 = -10.1250 \left(\frac{\alpha}{\pi} \right)^4 \tag{44}$$

as obtained from the three-loop $\overline{\text{MS}}$ calculation of the correlation function [10]. As a result of renormalization group scaling of the GSRs [3], the coupling in the perturbative coefficients is implicitly the running coupling at the scale $\nu^2 = \sqrt{\tau}$ in the $\overline{\text{MS}}$ scheme

$$\frac{\alpha(\nu^2)}{\pi} = \frac{1}{\beta_0 L} - \frac{\bar{\beta}_1 \log L}{(\beta_0 L)^2} + \frac{1}{(\beta_0 L)^3} [\bar{\beta}_1^2 (\log^2 L - \log L - 1) + \bar{\beta}_2] \quad (45)$$

$$L = \log \left(\frac{\nu^2}{\Lambda^2} \right) \quad , \quad \bar{\beta}_i = \frac{\beta_i}{\beta_0} \quad , \quad \beta_0 = \frac{9}{4} \quad , \quad \beta_1 = 4 \quad , \quad \beta_2 = \frac{3863}{384} \quad (46)$$

with $\Lambda_{\overline{\text{MS}}} \approx 300 \text{ MeV}$ for three active flavours, consistent with current estimates of $\alpha(M_\tau)$ [1].

The condensate contributions in (41), (42) involve next-to-leading order [12] contributions⁴ from the dimension four gluon condensate $\langle J \rangle$ and leading order [13] contributions from gluonic condensates of dimension six and eight

$$\langle \mathcal{O}_6 \rangle = \langle g f_{abc} G_{\mu\nu}^a G_{\nu\rho}^b G_{\rho\mu}^c \rangle \quad (47)$$

$$\langle \mathcal{O}_8 \rangle = 14 \left\langle \left(\alpha f_{abc} G_{\mu\rho}^a G_{\nu\rho}^b \right)^2 \right\rangle - \left\langle \left(\alpha f_{abc} G_{\mu\nu}^a G_{\rho\lambda}^b \right)^2 \right\rangle \quad (48)$$

$$b_0 = 4\pi \frac{\alpha}{\pi} \left[1 + \frac{175}{36} \frac{\alpha}{\pi} \right] \quad , \quad b_1 = -9\pi \left(\frac{\alpha}{\pi} \right)^2 \quad , \quad c_0 = 8\pi^2 \left(\frac{\alpha}{\pi} \right)^2 \quad , \quad d_0 = 8\pi^2 \frac{\alpha}{\pi} \quad . \quad (49)$$

The remaining terms in the GSRs (41), (42) represent instanton contributions obtained from single instanton and anti-instanton [11] (*i.e.*, assuming that multi-instanton effects are negligible [14]) contributions to the scalar gluonic correlator [5, 6, 13, 15]. The quantity ρ is the instanton radius, $n(\rho)$ is the instanton density function, and J_2 and Y_2 are Bessel functions in the notation of [16].

The instanton contributions to the Gaussian sum-rules can be interpreted [6] as naturally partitioning into an instanton continuum portion devolving from

$$\frac{1}{\pi} \text{Im} \Pi^{inst}(t) = -16\pi^3 \int d n(\rho) \rho^4 t^2 J_2(\rho\sqrt{t}) Y_2(\rho\sqrt{t}) \quad (50)$$

and a contribution which, like the $\Pi(0)$ low-energy theorem (LET) term, appears only in the $k = -1$ sum-rule

$$-\frac{128\pi^2}{\sqrt{4\pi\tau}} \exp\left(\frac{-\hat{s}^2}{4\tau}\right) \int d n(\rho) \quad . \quad (51)$$

This asymmetric role played by the instanton is crucial in obtaining a consistent analysis from these two sum-rules. In the absence of instanton contributions the LET tends to dominate the left-hand side of (22), corresponding to a massless state in the single-narrow resonance model (28). However, the higher-weighted sum-rules are independent of the LET, and in the absence of instantons lead to a much larger mass scale in sum-rule analyses. This discrepancy between the LET-sensitive and LET-insensitive sum-rules has

⁴The calculation of next-to-leading contributions in [12] have been extended non-trivially to $n_f = 3$ from $n_f = 0$, and the operator basis has been changed from $\langle \alpha G^2 \rangle$ to $\langle J \rangle$.

been shown to be resolved when instanton contributions are included in the Laplace sum-rules [5, 6]. A similar qualitative behaviour emerges from the Gaussian sum-rules, since the LET term in (22) and the LET-like instanton contribution (51) have the same functional form [*i.e.*, each is proportional to $\exp(-\hat{s}^2/(4\tau))$] and occur with opposite sign in the left-hand side of (22). Thus there exists a cancellation between these effects, which is easily verified as being significant in the instanton liquid model [17]

$$n(\rho) = n_c \delta(\rho - \rho_c) \quad (52)$$

$$n_c = 8.0 \times 10^{-4} \text{ GeV}^4 \quad , \quad \rho_c = \frac{1}{0.6} \text{ GeV}^{-1} \quad , \quad (53)$$

along with a standard value for the gluon condensate [18]

$$\langle \alpha G^2 \rangle = (0.07 \pm 0.01) \text{ GeV}^4 \quad . \quad (54)$$

This qualitative argument is upheld by the detailed GSR analysis presented in [4]. However, the $k = -1$ GSR analysis is more sensitive to QCD uncertainties, justifying a focus on the $k = 0$ GSR for the remainder of this paper.

6 Gaussian Sum-Rule Analysis of Scalar Gluonium

A single narrow resonance model analysis of the $k = 0$ Gaussian sum-rule results in a mass scale of approximately 1.3 GeV, but leads to poor agreement between the phenomenological model and QCD prediction as shown in Figure 3, indicating that the gluonium spectral function is poorly described by a single narrow resonance. Furthermore, in the narrow width model the second-order moment combination (39) should satisfy

$$\sigma_0^2 - 2\tau = 0 \quad , \quad (55)$$

but Figure 4 shows a substantial deviation from this behaviour [4]. Since this moment combination is related to the width of the GSR, we conclude that the gluonium resonance strength must be distributed over a significant energy range.

The clear failure of the single narrow resonance model, indicative of distributed resonance strength significant enough to be resolved by the GSRs, is a significant conclusion in its own right, but various distributed resonance strength models have also been analyzed [4]. In order of increasing number of parameters (and increasing complexity) they are

1. Single non-zero width models (2 parameters: mass, width)
2. Two narrow resonance model (3 parameters: two masses, relative resonance strength)
3. Narrow resonance plus a non-zero width resonance models (4 parameters: two masses, one width, relative resonance strength)

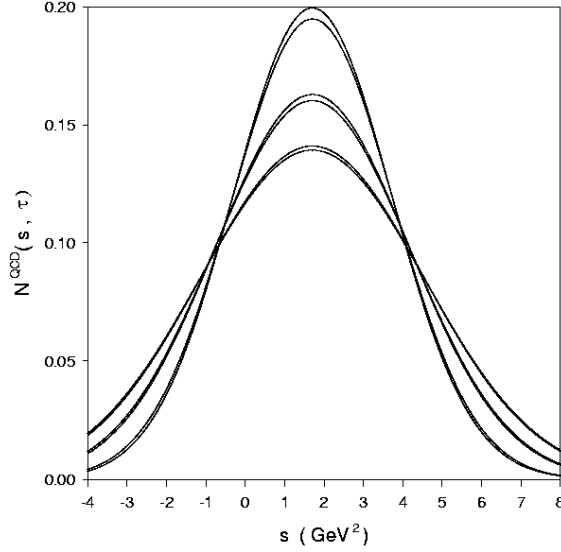


Figure 3: Comparison of the theoretical prediction for $N_0^{QCD}(\hat{s}, \tau, s_0)$ with the single narrow resonance phenomenological model. The τ values used for the three pairs of curves, from top to bottom in the figure, are respectively $\tau = 2.0 \text{ GeV}^4$, $\tau = 3.0 \text{ GeV}^4$, and $\tau = 4.0 \text{ GeV}^4$. Note the prominent disagreement between the QCD prediction and phenomenological model in the vicinity of the peaks.

In the single non-zero width models, elaborations on the square pulse include a Gaussian resonance and a skewed Gaussian resonance models

$$\rho(t) \sim \exp \left[-\frac{(t - m^2)^2}{2\Gamma^2} \right] \quad (56)$$

$$\rho(t) \sim t^2 \exp \left[-\frac{(t - m^2)^2}{2\Gamma^2} \right] \quad (57)$$

which are analytically and numerically simpler to analyze than a Breit-Wigner shape. In the Gaussian resonance models, the quantity Γ can be related to an equivalent Breit-Wigner width by $\Gamma_{BW} = \sqrt{2 \log 2} \Gamma / m$, and the t^2 factor in the skewed Gaussian is chosen for consistency with (low-energy) two-pion decay rates [7, 19]. The relevant moment combinations for the Gaussian model (56) are [4]

$$\frac{M_{0,1}}{M_{0,0}} = m^2 + \Gamma \Delta \quad (58)$$

$$\sigma_0^2 - 2\tau = \Gamma^2 - m^2 \Gamma \Delta - \Gamma^2 \Delta^2 \quad (59)$$

$$A_0^{(3)} = (m^4 \Gamma - \Gamma^3) \Delta + 3m^2 \Gamma^2 \Delta^2 + 2\Gamma^3 \Delta^3 \quad (60)$$

where

$$\Delta = \sqrt{\frac{2}{\pi}} \left[\frac{\exp \left(-\frac{m^4}{2\Gamma^2} \right)}{1 + \operatorname{erf} \left(\frac{m^2}{\sqrt{2}\Gamma} \right)} \right] \quad (61)$$

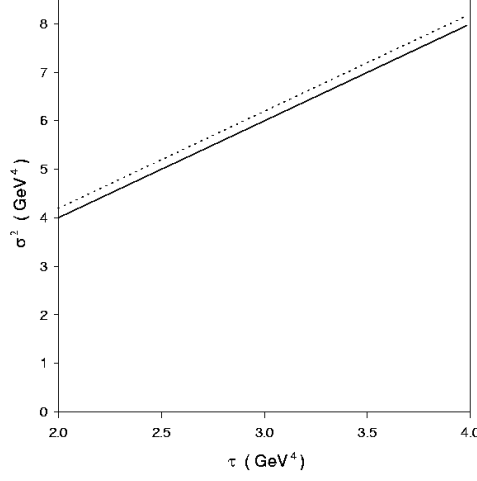


Figure 4: Plot of σ_0^2 for the theoretical prediction (dotted curve) compared with $\sigma_0^2 = 2\tau$ for the single-resonance model (solid curve) for the $k = 0$ sum-rule.

The quantity Δ is small, so the Gaussian model cannot accommodate large values of the asymmetry $A_0^{(3)}$. However, the skewed Gaussian naturally leads to a larger asymmetry as reflected in the following results for the relevant moment combinations [4]

$$\frac{M_{0,1}}{M_{0,0}} = \frac{m^2(m^4 + 3\Gamma^2)}{m^4 + \Gamma^2} + \mathcal{O}(\Delta) \quad (62)$$

$$\sigma_0^2 - 2\tau = \frac{\Gamma^2(m^8 + 3\Gamma^4)}{(m^4 + \Gamma^2)^2} + \mathcal{O}(\Delta) \quad (63)$$

$$A_0^{(3)} = \frac{4m^2\Gamma^6(m^4 - 3\Gamma^2)}{(m^4 + \Gamma^2)^3} + \mathcal{O}(\Delta) \quad . \quad (64)$$

The results for the single non-zero resonance models are shown in Table 1, and indicate that the non-zero width models underestimate the QCD value of the asymmetry $A_0^{(3)}$ by at least an order of magnitude [4]. This failure suggests that further phenomenological models which can generate a larger asymmetry are required.

	mass (GeV)	width (GeV)	$A_0^{(3)}$ (GeV ⁶)
square pulse	1.30 ± 0.17	0.59 ± 0.07	0
unskewed gaussian	1.30 ± 0.17	0.40 ± 0.05	0.000342
skewed gaussian	1.17 ± 0.15	0.49 ± 0.06	0.00943
QCD	—	—	-0.0825

Table 1: The results of a $k = 0$ Gaussian sum-rules analysis of a variety of non-zero resonance width models. The quoted resonance parameters include uncertainties introduced by the QCD input parameters, except for $A_0^{(3)}$ which is obtained from the central values. For the Gaussian resonance models, the given width is the equivalent Breit-Wigner width

A model containing two narrow resonances

$$\rho^{\text{had}}(t) = \pi [f_1^2 \delta(t - m_1^2) + f_2^2 \delta(t - m_2^2)] \quad (65)$$

results in the following normalized Gaussian sum-rule (26)

$$N_0^{\text{QCD}}(\hat{s}, \tau, s_0) = \frac{1}{\sqrt{4\pi\tau}} \left\{ r_1 \exp \left[-\frac{(\hat{s} - m_1^2)^2}{4\tau} \right] + r_2 \exp \left[-\frac{(\hat{s} - m_2^2)^2}{4\tau} \right] \right\} \quad (66)$$

where

$$r_1 = \frac{f_1^2}{f_1^2 + f_2^2}, \quad r_2 = \frac{f_2^2}{f_1^2 + f_2^2}, \quad r_1 + r_2 = 1 \quad (67)$$

parameterize the relative strength of the two resonances. This model can accommodate a large asymmetry parameter through an asymmetric distribution of resonance strength, as indicated by the following moment combinations [4]

$$\frac{M_{0,1}}{M_{0,0}} = \frac{1}{2}(z + ry) \quad (68)$$

$$\sigma_0^2 - 2\tau = \frac{1}{4}y^2(1 - r^2) \quad (69)$$

$$A_0^{(3)} = -\frac{1}{4}ry^3(1 - r^2) \quad (70)$$

$$S_0 - 12\tau^2 - 12\tau(\sigma_0^2 - 2\tau) = \frac{1}{16}y^4(1 - r^2)(1 + 3r^2), \quad (71)$$

where

$$z = m_1^2 + m_2^2, \quad y = m_1^2 - m_2^2, \quad r = r_1 - r_2 \quad (72)$$

$$S_0 \equiv \frac{M_{0,4}}{M_{0,0}} - 4\frac{M_{0,3}}{M_{0,0}}\frac{M_{0,1}}{M_{0,0}} + 6\frac{M_{0,2}}{M_{0,0}}\left(\frac{M_{0,1}}{M_{0,0}}\right)^2 - 3\left(\frac{M_{0,1}}{M_{0,0}}\right)^4. \quad (73)$$

The lowest three moment combinations (68)–(70) are used to determine the three resonance parameters, and the final fourth-order residual combination (71) is used as a test of the agreement between QCD and the phenomenological model. The resulting resonance parameters are [4]

$$m_1 = (0.98 \pm 0.2) \text{ GeV}, \quad m_2 = (1.4 \pm 0.2) \text{ GeV}, \quad r_1 = 0.28 \mp 0.06, \quad r_2 = 1 - r_1. \quad (74)$$

Results from the fourth-order moment measure of the accuracy between QCD and the two-narrow resonance model is given in Table 2, and indicate an approximately 50% discrepancy between QCD and the phenomenological model [4].

As a final attempt to improve the agreement between the next-highest moment test of the agreement between QCD and the phenomenological model, consider a narrow resonance of mass m and relative strength r_m , combined with a second resonance of mass M , width Γ and relative strength r_M . Of course for a normalized GSR we must

	$S_0 - 12\tau^2 - 12\tau(\sigma_0^2 - 2\tau)$
QCD	0.170 GeV^8
double resonance model	0.074 GeV^8

Table 2: The results of a $k = 0$ Gaussian sum-rules analysis of the double narrow resonance model using central values of the QCD parameters.

have $r_m + r_M = 1$, so this defines a four-parameter model. For example, when a square pulse is used to describe the second resonance the resulting normalized GSR is

$$N_0^{\text{QCD}}(\hat{s}, \tau, s_0) = r_m \frac{1}{\sqrt{4\pi\tau}} \exp\left[-\frac{(\hat{s} - m^2)^2}{4\tau}\right] + r_M \frac{1}{4M\Gamma} \left[\text{erf}\left(\frac{\hat{s} - M^2 + M\Gamma}{2\sqrt{\tau}}\right) - \text{erf}\left(\frac{\hat{s} - M^2 - M\Gamma}{2\sqrt{\tau}}\right) \right], \quad (75)$$

where $r_m + r_M = 1$. Four moment combinations are then needed to define the resonance parameters, and a fifth-order moment combination serves as a measure of the agreement between QCD and the phenomenological model [4]

$$\frac{M_{0,1}}{M_{0,0}} = \frac{1}{2}(z + ry) + \mathcal{O}(\Delta) \quad (76)$$

$$\sigma_0^2 - 2\tau = \frac{1}{4}y^2(1 - r^2) + \frac{1}{12}\Gamma^2(z - y)(1 - r) + \mathcal{O}(\Delta) \quad (77)$$

$$A_0^{(3)} = -\frac{1}{4}y^3r(1 - r^2) - \frac{1}{8}\Gamma^2y(1 - r^2)(z - y) + \mathcal{O}(\Delta) \quad (78)$$

$$S_0 - 12\tau^2 - 12\tau(\sigma_0^2 - 2\tau) = \frac{1}{16}y^4(1 - r^2)(1 + 3r^2) + \frac{1}{8}\Gamma^2y^2(1 + r)(1 - r^2)(z - y) + \frac{1}{40}\Gamma^4(1 - r)(z - y)^2 + \mathcal{O}(\Delta) \quad (79)$$

$$A_0^{(5)} - 20\tau A_0^{(3)} = -\frac{1}{8}y^5r(1 - r^2)(1 + r^2) - \frac{5}{48}\Gamma^2y^3(1 - r^2)(1 + r)^2(z - y) - \frac{1}{16}\Gamma^4y(1 - r^2)(z - y)^2 + \mathcal{O}(\Delta) \quad (80)$$

where the fifth-order asymmetry moment is

$$A_k^{(5)} = \frac{M_{k,5}}{M_{k,0}} - 5\frac{M_{k,4}}{M_{k,0}}\frac{M_{k,1}}{M_{k,0}} + 10\frac{M_{k,3}}{M_{k,0}}\left(\frac{M_{k,1}}{M_{k,0}}\right)^2 - 10\frac{M_{k,2}}{M_{k,0}}\left(\frac{M_{k,1}}{M_{k,0}}\right)^3 + 4\left(\frac{M_{k,1}}{M_{k,0}}\right)^5. \quad (81)$$

The resulting resonance parameters and the QCD prediction and phenomenological values of the fifth-order asymmetry parameter are shown in Table 3 [4]. An interesting feature of the results are that the wide resonance is consistently found to be lighter than the narrow resonance, and that the narrow plus skewed Gaussian model shows only a 20% deviation from the QCD value of the fifth order asymmetry parameter.

	m (GeV)	M (GeV)	Width (GeV)	r_m	$A_0^{(5)} - 20\tau A_0^{(3)}$
square	1.33 ± 0.18	1.23 ± 0.18	0.95 ± 0.12	0.6 ± 0.13	-0.11 GeV^{10}
gauss	1.41 ± 0.19	1.23 ± 0.15	0.52 ± 0.06	0.49 ± 0.13	-0.13 GeV^{10}
skewed	1.38 ± 0.13	1.06 ± 0.21	0.69 ± 0.07	0.44 ± 0.04	-0.19 GeV^{10}
QCD	—	—	—	—	-0.24 GeV^{10}

Table 3: Resonance parameters obtained in the various two-resonance scenarios. The label “square” denotes the narrow plus square pulse model, “gauss” refers to narrow plus Gaussian resonance model, and “skewed” indicates the narrow plus skewed Gaussian model. The mass M denotes the state associated with the quoted width, which corresponds to the equivalent Breit-Wigner width for the Gaussian models. The quoted resonance parameters include uncertainties introduced by the QCD input parameters, except for the fifth-order residual moment combination which is obtained from the central values.

7 Comparison of Distributed Resonance Strength Models

All the distributed resonance strength models considered in the previous section lead to the excellent agreement between the QCD and phenomenological sides of the normalized GSR shown in Figure 5, and clearly resolve the discrepancy evident in Figure 3 corresponding to the single resonance model [4]. However, a χ^2 measure of the agreement between the theoretical and phenomenological curves in Figure 5 result in a χ^2 which is an order of magnitude smaller in the two-resonance models [4]. The combination of this result with the Table 1 observation of at least an order of magnitude disagreement with the QCD value of the third-order asymmetry is compelling evidence in favour of a two-resonance scenario for distributed resonance strength, with an upper bound on the heavier mass of about 1.6 GeV obtained from Eq. (74) and Table 3.

The various two-resonance models all have similar values of χ^2 , which does not provide a useful criteria to distinguish between these models. However, the narrow plus skewed Gaussian resonance model leads to the best ($\approx 20\%$) agreement with the QCD value of the next-order moment. In this scenario, the mass predictions and the pattern of a lighter broad resonance and a heavier narrow resonance is consistent with the identification of gluonium content in the $f_0(1370)$ and $f_0(1500)$.

8 Conclusions

In this paper, the formulation of Gaussian sum-rules has been reviewed. The key qualitative feature of Gaussian sum-rules is their enhanced sensitivity to excited states in comparison with Laplace sum-rules. Thus any resonance strong enough to stand out from the QCD continuum should reveal itself in a GSR analysis. The significance of normalized GSRs has been emphasized since they provide information independent of the the finite-energy sum-rule constraint that arises from the evolution of GSRs through the diffusion equation [3].

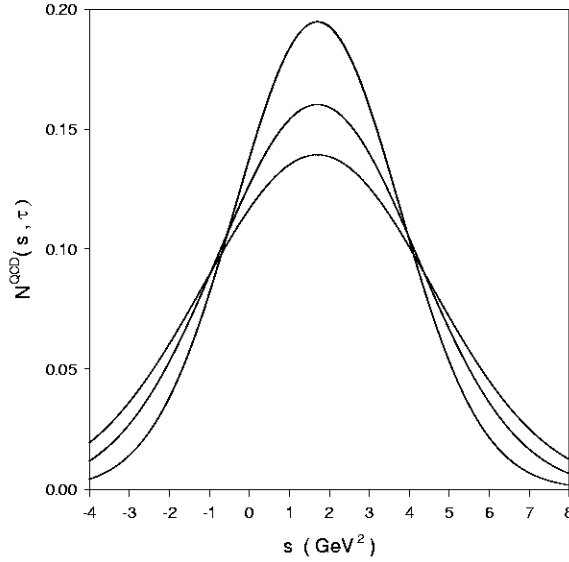


Figure 5: Comparison of the theoretical prediction for $N_0^{QCD}(\hat{s}, \tau, s_0)$ with the distributed resonance phenomenological models. The τ values used for the three pairs of curves, from top to bottom in the figure, are respectively $\tau = 2.0 \text{ GeV}^4$, $\tau = 3.0 \text{ GeV}^4$, and $\tau = 4.0 \text{ GeV}^4$. The almost perfect overlap between QCD and phenomenology is particularly impressive because there are no free parameters corresponding to the normalization of the QCD prediction and phenomenological models.

Methods for obtaining phenomenological predictions from GSRs have been reviewed and applied to the ρ meson to demonstrate the predictive power of GSRs [3]. These techniques are easily adapted to a variety of resonance models, and through combinations of GSR moments, provide a natural criterion for testing the accuracy of the phenomenological model in comparison with QCD [4].

The important role of instanton effects in relation to the low-energy theorem has been illustrated for the GSRs of scalar gluonic currents. This analysis provides additional support for the interpretation of instanton effects first developed for Laplace sum-rules [6]. An identical, and natural, partitioning of instanton effects into a continuum and LET-like contribution resolves discrepancies between the LET-sensitive and LET-insensitive sum-rules in both the Laplace and Gaussian sum-rules.

A detailed phenomenological analysis of the $k = 0$ GSR is presented because it is less sensitive to QCD parameter uncertainties than the $k = -1$ (LET-dependent) GSR. The analysis clearly rules out a single narrow resonance scenario, and further indicates that gluonium resonance strength is spread over a broad energy region. In particular, evidence exists for two resonances below $\approx 1.6 \text{ GeV}$ with a significant gluonium content, with the lighter resonance having a substantial width [4]. Such a scenario is consistent gluonium content of $f_0(1370)$ and $f_0(1500)$.

Acknowledgments:

TGS and DH are grateful for research funding from the Natural Sciences & Engineering Research Council of Canada (NSERC). Many thanks to Amir Fariborz and SUNY IT for careful organization and generous hospitality during the workshop on Theoretical High-Energy Physics.

References

- [1] K. Hagiwara *et al.*, Phys. Rev. **D66** (2002) 010001.
- [2] R.A. Bertlmann, G. Launer, E. de Rafael, Nucl. Phys. **B250** (1985) 61.
- [3] G. Orlandini, T.G. Steele and D. Harnett, Nucl. Phys. **A686** (261) 2001.
- [4] D. Harnett, T.G. Steele, Nucl. Phys. **A695** (2001) 205.
- [5] E.V. Shuryak, Nucl. Phys. **B203** (1982) 116;
H. Forkel, Phys. Rev. **D64** (2001) 034015.
- [6] D. Harnett, T.G. Steele, V. Elias, Nucl. Phys. **A686** (2001) 393.
- [7] V.A. Novikov, M.A. Shifman, A.I. Vainshtein and V.I. Zakharov, Nucl. Phys. **B191** (1981) 301.
- [8] V. Giménez, J. Bordes, J. Peñarrocha, Phys. Lett. **B223** (1989) 251;
S.N. Nikolaev, H.R. Radyushkin, Nucl. Phys. **B213** (1983) 285;
D.J. Broadhurst, S.C. Generalis, Phys. Lett. **B165** (1985) 175.
- [9] V. Giménez, J. Bordes, J. Peñarrocha, Nucl. Phys. **B357** (1991) 3.
- [10] K.G. Chetyrkin, B.A. Kneihl and M. Steinhauser, Nucl. Phys. **B510** (1998) 61.
- [11] A. Belavin, A. Polyakov, A. Schwartz and Y. Tyupkin, Phys. Lett. **B59** (1975) 85;
G. 't Hooft, Phys. Rev. **D14** (1976) 3432.
- [12] E. Bagan and T.G. Steele, Phys. Lett. **B234** (1990) 135.
- [13] V.A. Novikov, M.A. Shifman, A.I. Vainshtein and V.I. Zakharov, Nucl. Phys. **B165** (1980) 67.
- [14] T. Schäfer and E.V. Shuryak, Phys. Rev. Lett. **75** (1995) 1707.
- [15] B.V. Geshkenbein and B.L. Ioffe, Nucl. Phys. **B166** (1980) 340;
B.L. Ioffe and A.V. Samsonov, Phys. of Atom. Nucl. **63** (2000) 1527.
- [16] M. Abramowitz and I.E. Stegun, *Mathematical Functions with Formulas, Graphs, and Mathematical Tables* (National Bureau of Standards Applied Mathematics Series, Washington) 1972.

- [17] E.V. Shuryak, Nucl. Phys. **B203** (1982) 93.
- [18] S. Narison, Nucl. Phys. B (Proc. Supp.) **54A** (1997) 238.
- [19] V.A. Novikov, M.A. Shifman, Z. Phys. **C8** (1981) 43;
M.A. Shifman, Z. Phys. **C9** (1981) 347.